Numerical Methods in Civil Engineering

Optimization of Reservoir Operation using a Bioinspired Metaheuristic Based on the COVID-19 Propagation Model

Alireza Donyaii*, Amirpouya Sarraf**

ARTICLE INFO

Article history:
Received:
July 2020.
Revised:
August 2020.
Accepted:
August 2020.

Keywords:
Bias Correction Spatial Disaggregation, Climate Change, Coronavirus Optimization Algorithm, Extreme Learning Machine, MIROC-ESM, Voshmgir Dam Reservoir.

Abstract:

Recently, global warming problems with rapid population growth and socio-economic development have intensified the demand for water and increased tensions on water supplies. This research evolves the Multi-Objective Coronavirus Optimization Algorithm (MOCVOA) to obtain operational optimum rules of Voshmgir Dam reservoir under the climate change conditions. The climatic variables downscaled and predicted by the Bias Correction Spatial Disaggregation (BCSD) method of MIROC-ESM model, was introduced into the Extreme Learning Machine (ELM) modelto evaluate the future runoff flowing into the reservoir. The model objective functions included minimizing vulnerability and enhancing reliability indices during baseline and climate change periods. Results revealed that under climate change conditions, the river flow would decrease by 0.17%, increase the temperature up to 2°C and decrease the rainfall by 23.8%, corresponding to the baseline period. Moreover, the extent of vulnerability index variations in the baseline and climate change conditions were also determined as 20-38% and 13-40%, respectively. The reliability index changes under the baseline and climate change conditions obtained were, 57-85% and 40-91%. Therefore, the vulnerability index was also measured at 33% and 30% for baseline and climate change conditions, respectively, with 80% of reliability index. Finally, the comparison of reservoir performance in meeting the water needs of downstream lands at the Pareto point of 80% reliability under both conditions indicated that the reservoir release rate would be more in line with the demand in the climate change conditions.

1. Introduction

Observed variations in global temperature, duration and severity of heat waves or droughts, changes in precipitation frequency or its intensity, decreased snow cover, rapid melting of ice and variations in soil moisture and runoff are some of the main recorded hydrological modifications frequently associated with global climate change. Due to the interactive relationship of hydrological variables (Huntington, 2006)[1], changes in precipitation and evaporation will affect river flows (Loaiciga et al. 1996; Muzik, 2001; Boyer et al., 2010) [2, 3, and 4], the frequency and intensity of droughts or floods (Bronstertet al., 2007) [5] and the amount of water supply.

Water resources management will then be faced with significant adversities(Jiang et al., 2007; Georgakakoset al. 2012; Hariri-Ardebili et al. 2019)[6, 7, and 8]. Therefore, agricultural water management, which depends concurrently on precipitation, evaporation and river flow, will be affected significantly (Yang et al. 2013; Nam and Choi, 2014; and Mirzabozorg et al. 2014)[9, 10 and 11].

Reservoirs are one of the most effective primary infrastructure elements for combining water resources development and management (Loucks and van Beek, 2005; Li et al., 2010; Liu et al. 2011, Liu et al. 2015)[12, 13, 14 and 15] .

**Ph.D. in Civil Engineering, Water Resources Expert, Golestan Regional Water Company, Gorgan, Iran.*

*** Corresponding Author: Assistant Professor of Civil Engineering Department, Roudehen Branch, Islamic Azad University, Roudehen, Iran.*
Email: sarraf@riau.ac.ir

Within the limitations of the available water resources, the irrigation reservoir has become increasingly critical for sustainable agriculture.

Many studies related to irrigation reservoir operations were primarily performed in the 1990s (Vedula and Kumar, 1996; Mujumdar and Ramesh, 1997; Umamahesh and Sreenivasulu, 1997; Hajilal et al., 1998)[16, 17, 18 and 19].

The techniques related to irrigation reservoir operation include particularly linear programming (Haddad et al., 2009; Singh, 2015)[20], non-liner programming (Consoli et al., 2008)[21], dynamic programming (Umamahesh and Sreenivasulu, 1997; Teixeira and Marino, 2002; Prasad et al., 2013)[18, 22 and 23], evolution optimization algorithm (Reddy and Kumar, 2007)[24] and other approaches.

The climate change effects on reservoir operations are also well known by researchers of water resources. As a result, a variety of adaptive techniques have been created to minimize possible adverse effects of climate change. There is a great deal of literature underlining adaptation to the agricultural irrigation reservoir. Shnaydman (1993)[25] addressed the effect of climate change on the efficiency strategy of the Irrigation water resources System (WRS) and applied a simulation model with a water supply delivery algorithm between users and a WRS operation with stochastic water requirements.

Georgiou and Papamichail (2008)[26] have developed a non-linear programming optimization model for an optimized soil water equilibrium under four climate change scenarios, which aims to define optimal reservoir release policies, multi-crop irrigation allocation and optimal irrigated crop patterns.

Ncube et al. (2011)[27] analyzed reservoir operation under variable climate scenarios, including decreased water supply caused by climate change but with growing annual demands, and climate change conditions combined with improvements in irrigation technologies.

Nam and Choi (2014)[10] suggested an irrigation vulnerability assessment strategy, considering the probability distribution that uses time-dependent change assessments of paddy irrigation water and reservoir capacity requirements.

Afkhamifar & Sarraf[28] evaluated The efficiency of two models of Extreme Learning Machines (ELM), Artificial Neural Network (ANN) and the combination of two models with wavelet propagation algorithms (W-ELM and W-ANN). Their results showed that the W-ELM-QPSO hybrid model had a high speed in terms of training and testing speed in addition to forecasting power compare to other models .

Donyaii et al. (2020a) [29] developed the Multi-Objective Grey Wolf Optimization (MOGWO) algorithm to obtain the optimum rules in operation of Golestan Dam reservoir in Golestan province, Iran, under climate change conditions. The results showed that the river flow would decline by 0.17 percent of the baseline period under climate change conditions in addition to increasing the temperature by 20% and decreasing the rainfall by 21.1%.

In another research in the same year, they studied the Multi-Objective Farmland Fertility Optimization (MOFFA) algorithm to derive optimum rules on the operation of the Golestan Dam under climate change conditions. The study results indicated an increase in release rates for climate change conditions in comparison with the baseline ones and stronger dam efficiency in climate change conditions (Donyaii et al. 2020b) [30].

The present study suggested the development and application of the multi-objective coronavirus optimization algorithm (MOCVOA) as an innovative methodology of water management, which was not addressed in previous studies.

In addition, the optimum operating rules of the Voshmgir Dam reservoir (Golestan Province, Iran) under baseline conditions (April 2007 to October 2019) and climate change conditions (April 2040 to October 2052) using the MOCVOA algorithm, with two objectives of minimizing vulnerability and maximizing the demand-supply reliability index, were defined and compared as required during those periods.

The techniques used in this study are as follows:

(i) Assessing parameters for climate change conditions;

(ii) Simulation of rainfall-runoff processes to determine the water volume entering Voshmgir Dam;

(iii) Assessment of baseline and climate change conditions water demand volume as well as extracting the multi-objective operating rules (based on three variables of storage volume, demand volume, and release from the reservoir) in climate change and baseline conditions

Finally, the protocols for this study are to correlate the optimal allocation strategies with the performance measures and efficiency indices of the reservoir under baseline and climate change conditions.

2. Materials and methods

2.1. Downscaling of climate change parameters

In this study, in order to investigate the climate change effects on the hydro-climatological variables of Gorganroud watershed, the downscaled output obtained from the Bias Correction Spatial Disaggregation (BCSD)[31] method of MIROC-ESM model was used.

The results showed an increase in the average monthly temperature by 1.9 to 2.2 °C in all climate change scenarios. Examination of monthly average rainfall changes also showed that the decrease in precipitation rate in the future period is quite evident, and according to the average scenario, it can be amounted to 23.8% less than the baseline period.

2.2 Rainfall-runoff simulation

The Extreme Learning Machine (ELM) model proposed by Huang et al. (2005) [32] was used to evaluate the impact of climate change phenomenon on the runoff flowing into the reservoir. Thus, the predicted rainfall-runoff data was determined by entering the output data of the climate change simulations into the ELM.

In the next step, after determining the irrigation requirement for future crops based on a constant agricultural region, the amount of irrigation demand was calculated for the different months of the future period.

In addition, the cultivation and reference evapotranspiration detection was executed by using the FAO and the Penman-Monteith FAO techniques.

2.3 Extreme Learning Machine

Extreme learning machine has an extremely fast train stage with a high generalization performance. High train speed is based on picking up the input weights and biases randomly and calculating the output weights analytically. The main differences between ELM and traditional gradient based learning algorithms for feed-forward neural networks are as follows [32]:

- The ELM has an extremely fast learning stage.
- The ELM tends to reach the solutions straightforward without trivial issues, such as local minima, learning rate, momentum rate and over-fitting encountered in traditional gradient based learning algorithm.
- ELM algorithm can be used to train single layer feed forward networks (SLFN) using several non-differentiable activation functions [32].

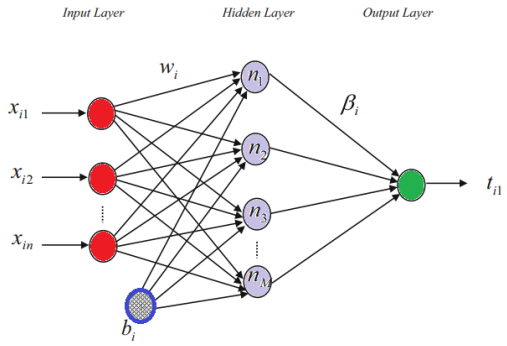

Fig. 1: SLFN Network Architecture

ELM is a kind of algorithm with higher efficiency which is easy to implement, and contains three layers namely; input layer, hidden layer and output layer [Guo et al. 2009, Zhu et al. 2005] [33 and 34]. Figure 1 shows the architecture of ELM which contains n input neurons, l hidden neurons and m output neurons.

For N different learning samples $(x_i, y_i) \in R_n \times R_m$, (i=1,2,…, N), the output of hidden layer can be expressed as equation(1), and the output of neuron in output layer can be expressed as equation(2).

$$h = g(wx + b) \tag{1}$$

$$h_{(x_i)}\beta = Y_i^T \ , \qquad i = 1, 2, \dots, N \tag{2}$$

Where g(x) expresses hidden layer activation function of ELM, β is the weight between output and hidden layer, w is the weight between hidden layer and input layer, and b is the bias of hidden neuron.

H represents the connection matrix between hidden layer and output layer, Y indicates the training data target matrix, so, equation (2) can be transformed as:

$$H = \begin{bmatrix} g(w_1, b_1, x_1)g(w_2, b_2, x_1) \dots g(w_l, b_l, x_1) \\ g(w_1, b_1, x_2)g(w_2, b_2, x_2) \dots g(w_l, b_l, x_2) \\ \vdots \\ g(w_1, b_1, x_N)g(w_2, b_2, x_N) \dots g(w_l, b_l, x_n) \end{bmatrix}_{N \times l},$$

$$\beta = \begin{bmatrix} \beta_1^T \\ \beta_2^T \\ \vdots \\ \beta_l^T \end{bmatrix}_{l \times m}, \tag{3}$$

$$Y = \begin{bmatrix} Y_1^T \\ Y_2^T \\ \vdots \\ Y_l^T \end{bmatrix}_{N \times m}$$

If g (wi, bi, xj) was infinitely differentiable, the network only needs to set the number of hidden layer nodes, without the need to adjust the input weights and the bias of hidden layer [Huang et al. (2005), Huang and Siew (2006)] [32 and 35]. Before training of ELM, it determines the number of input layer neurons based on the sample feature vectors and establishes the number of output layer neurons based on the sample categories, according to the specific conditions to determine the activation function and the number of hidden layer neurons [Huang et al. (2006)] [36]. As ELM can randomly generate w and b before training,-it confirms the number of hidden layer neurons and the activation function of the hidden layer neurons, and then

calculates using the least squares. The whole process finishes in one single time without iterations, so it is significantly fast. The following steps are the main training processes of ELM:

Step 1: Determine the number of hidden layer neurons, randomly set bias b of hidden layer neurons, and set weights w between input layer and hidden layer;

Step 2: Choose an infinitely differentiable function as the activation function, and then calculate the hidden layer output matrix H;

Step 3: Calculate weights β between hidden layer and output layer: $\beta = H^T H$, where H^T is the generalized inverse matrix of the output matrix H (Ding et al. 2017)[37].

In the present study, the Extreme Learning Machine (ELM) method was used to simulate the future runoff under the climate change conditions at the inlet of Voshmgir Dam, due to its better performance compared to other conventional methods. In this regard, to evaluate the different models used in the rainfall-runoff simulation process, the parameters of error, correlation coefficient and Nash-Sutcliffe coefficient were used. According to the results, the best simulation model was characterized with the correlation and Nash-Sutcliffe coefficients of 98% and 95%, respectively.

2.4 Operation models of Voshmgir reservoir

The Quantitative Control Models were proposed in order to provide opportunities to evaluate the optimization of water resources systems or the optimal allocation of limited water resources. Problems are converted into a numerical model for processing optimization strategies of decision-making problems to achieve the preferred objectives. Decision variables act as possible alternatives in the decision-making phase in the numerical model (Shokri et al. 2013). [38]

The objective function of the drawbacks of irrigation allocation is described as a minimization of the average squared relative irrigation allocation shortage. Moreover, the equations (4 to 9) define both the objective function and its constraints. (Ashofthe et al. 2013) [39].

$$\text{Minimize } F_{(d)} = 1/T \sum_{t=1}^{T} \left(\frac{De_t - Re_t}{De_{max}}\right)^2 \quad \forall_t = 1, 2, \dots, TT \tag{4}$$

$$S_{t+1} = S_t + Q_t - Re_t - Sp_t - (\bar{A}_t . Ev_t) \quad \forall_t = 1, 2, \dots, T \tag{5}$$

$$\bar{A}_t = c_0 + c_1 \bar{S}_t \tag{6}$$

$$S_{P_t} = \begin{cases} S_t + Q_t - Re_t - (\bar{A}_t . Ev_t) - S_{max} \\ \text{if } S_t + Q_t - Re_t - (\bar{A}_t . Ev_t) \geq S_{max} \\ 0 \\ \text{if } \quad S_t + Q_t - Re_t - (\bar{A}_t . Ev_t) < S_{max} \end{cases} \tag{7}$$

$$S_{min} \leq S_t \leq S_{max} \forall_t = 1, 2, \dots, T \tag{8}$$

$$0 \leq Re_t \leq De_{max} \forall_t = 1, 2, \dots, T \tag{9}$$

In which,

$F_{(d)}$= the objective function of irrigation allocation,

De_t= the total amount of irrigation demand through interval t,

Re_t = the water release through interval t.

De_{max} = the maximum amount of irrigation demand for the whole length of the planning duration,

Q_t = the inflow volume to the reservoir for interval t,

Ev_t = the net evaporation of the reservoir through interval t.

$\bar{A}_t$= the average reservoir surface area at the start and ending of interval t.

$\bar{S}_t$ = the average reservoir storage volume at the start and end of interval t,

S_{max} = the maximum volume of the reservoir,

S_{min} = the minimum volume of the reservoir,

S_{P_t} = the overflow volume of the reservoir in interval t,

T = the total time interval of the plan, and c_0 and c_1 are the constants in the surface-volume curve of the reservoir.

S_t and S_{t+1} are the reservoir storage volumes at the start and end of interval t, respectively.

The following penalty functions will be applied to the objective function in case of a violation of the constraints in Equations (8) and (9) (Ashofteh et al. 2013) [39]:

$$Pf_{1t} = a' . \left(\frac{|S_{min} - S_t|}{S_{max} - S_{min}}\right)^2 + b' \quad \forall_t = 1, 2, \dots, T \tag{10}$$

$$Pf_{2t} = c' . \left(\frac{Re_t - De_{max}}{De_{Max}}\right)^2 + d' \quad \forall_t = 1, 2, \dots, T \tag{11}$$

In which,

Pf_{1t} = the penalty function resulting from the constraint violation in equation (8), Pf_{2t} = the penalty functions resulting from constraint violation in equation (9). And a', b', c',$d'$are the non-negative constants in the penalty functions.

2.5 Operating Guidelines for the Reservoir

Typically, operating rules can be developed by using two strategies. The main methodology, referred to as the

implicit approach of stochastic optimization relies on historical time series (Karamouz et al. 1992) [40]. The primary methodology relies on the majority of regression equations that describe the relationships between independent and dependent variables. The following approach, called the explicit process of stochastic optimization (Loucks and Van Beek 2005) [12], uses the probabilities of transition between two successive stream flows. Normally, there are many kinds of rules, but at any particular time of the year, everyone needs the release of the reservoir or the necessary volume of storage.

These standards, for example, identify goals for storage volume, while others explain the detection of storage areas relevant to a specific release strategy (Loucks and Van Beek 2005) [12].

The second method used in the analysis is based on decision parameters, such as the reservoir inflow volume, the storage volume and the downstream water demand volume of the reservoir to fulfill the irrigation needs as follows (Ashofteh et al. 2013) [39]:

$$\mathrm{Re}_t = \mathrm{f}(\mathrm{Q}_t, \mathrm{S}_t, \mathrm{De}_t) \forall_t = 1, 2, \dots, T \quad (12)$$

In which,

Re_t, Q_t, S_t, and De_t are the release, inflow, storage volume, and downstream irrigation demand for time t, respectively.

$\mathrm{f}(\mathrm{Q}_t, \mathrm{S}_t, \mathrm{De}_t)$=the rule curve derived by MOCVOA algorithm.

2.6 Efficiency Indices of Reservoir

To evaluate the performance of the reservoir operation, various efficiency indices may be added. Based on the issue type and the aim of the planning process, efficiency indices may be different. Equations (13-14), produce and represent indices of reliability and vulnerability respectively (Ashofteh et al. 2013) [39].

If the purpose of the reservoir is to provide the requirements for irrigation, the reliability indicator will be specified as equation (13) [39].

$$\alpha = \frac{\mathrm{N}_{t=1}^{\mathrm{T}}(\mathrm{De}_t \le \mathrm{Re}_t)}{\mathrm{T}} \quad (13)$$
$$\forall_t = 1, 2, \dots, T$$

In which,

α = the reliability index,

$\mathrm{N}_{t=1}^{\mathrm{T}}(\mathrm{De}_t \le \mathrm{Re}_t)$ = the amount of time intervals during which demand is provided.

As stated in equation (14), the vulnerability indicator is defined as the relative sum of the total system failure magnitude to the total volume of irrigation demand [39].

$$\vartheta = \frac{\sum_{t=1}^{\mathrm{T}}(\mathrm{De}_t - \mathrm{Re}_t | \mathrm{De}_t > \mathrm{Re}_t)}{\sum_{t=1}^{\mathrm{T}} \mathrm{De}_t} \quad (14)$$
$$\forall_t = 1, 2, \dots, T$$

In which,

ϑ = the vulnerability indicator,

$\sum_{t=1}^{\mathrm{T}}(\mathrm{De}_t - \mathrm{Re}_t | \mathrm{De}_t > \mathrm{Re}_t)$= the cumulative deficits in the overall time period,

$\sum_{t=1}^{\mathrm{T}} \mathrm{De}_t$ = the total demand for irrigation over the entire time period.

2.7 Coronavirus Optimization Algorithm

Severe acute respiratory syndrome coronavirus (SARS-CoV-2) is a new respiratory virus that causes 2019 coronavirus disease (COVID-19), first detected in humans in December 2019. It has spread worldwide, reportedly infecting more than 4 million people so far [41]. Much of the virus remains unclear, such as, how many people may have very mild, asymptomatic, or simply undocumented infections. It is difficult to determine the exact measurements of the outbreak [42].

Bioinspired models usually imitate behaviors from nature and are known to find parameters in machine learning model optimization for their efficient use in hybrid approaches [43]. Viruses can infect individuals and these individuals can die, infect other individuals, or simply recover after the disease. Usually, vaccines and the immune defense system combat the disease and help to mitigate its symptoms when a person remains infected. Usually, this behavior is modeled by a SIR model composed of three categories of people; S for the number of susceptible people, I for the number of infectious people, and R for the number of recovered people.

Evolutionary algorithms must deal with enormous search spaces, even infinite, for continuous cases, and must find suboptimal solutions in reasonable execution times [44]. The rapid spread of the coronavirus and its potential to cause infection at a very fast pace in most countries in the world, have inspired the novel metaheuristic applied in this paper, called the coronavirus optimization algorithm (CVOA). Regarding other similar approaches, the main CVOA characteristics can be summarized as follows:

(1) The scientific community is not currently aware of accurate coronavirus statistics and some aspects, such as the reinfection rate, are still controversial. In this sense, several problems such as the absence of tests for asymptomatic individuals, the infection rate, mortality rate, spreading rate, or reinfection probability could not be accurately estimated so far. However, as reported by the World Health Organization (WHO), the current state of the pandemic suggests certain values. [45]. Consequently, CVOA is parameterized for rates and probabilities with the actual reported values, preventing the user from performing an additional study on the most appropriate setup configuration.

(2) After several iterations, CVOA was able to stop the solution exploration, without need to configure it. That is, over the first iterations, the number of infected individuals increases; however, the number of infected individuals begins to decrease after a certain number of iterations, until reaching a void infected set of individuals.
(3) The high spreading rate of the coronavirus is useful for exploring promising regions more thoroughly (intensification), while the use of parallel strains ensures that all regions of the search space are equally explored (diversification).
(4) The proposal for a new discrete and dynamic length codification specifically designed to combine long-term short-term memory (LSTM) networks with CVOA (or any other metaheuristic) is another relevant contribution to this study.
The methodology of CVOA will be introduced in this section, where the steps section outlines the phases for a single pressure. The Proposed Parameters Configuration section illustrates how you need to configure the input parameters, and the section on pseudocodes contains the CVOA pseudocodes [46].

2.8 STEPS

Step 1. **initial population generation**. One person, the so-called patient-zero (PZ), consists of the initial population. It recognizes the first human being infected, as in the coronavirus pandemic. A random initialization for the PZ is proposed if no previous local minimum has been detected.

Step 2. **Propagation of Disease**. Several cases are judged based on the person [46]:
(1) In conjunction with the COVID-19 death rate, each infected person has a risk of dying(PDIE). The disease will not be transmitted to new individuals by those persons.
(2) The individuals who do not die will cause new individuals to become infected (intensification). According to a given probability, two forms of propagation are considered (PSUPERSPREADER):

(a) **Ordinary propagators**. According to a normal propagation rate(SPREADINGRATE), infected individuals would infect new individuals
(b) **Super-spreaders**. According to a super-spreading rate(SUPERSPREADINGRATE), infected individuals can infect new individuals.

(3) There is another factor to be considered, as diversification has to be ensured. In the searching space, both ordinary and super-spreader individuals will travel and discover very different solutions. Individuals are also expected to travel (PTRAVEL) to spread the disease to solutions that could be quite different(TRAVELERRATE). In case of not being a traveler, new solutions will change according to an ORDINARYRATE. Notice that super-spreaders and travelers may all be one person.

Step 3. population Updating. Three populations are maintained and updated for each generation [46].

(1) **Deaths**. Dead individual should be added to this population and can never be used again.
(2) **Recovered Population**. Infected individuals (after distributing the coronavirus according to the previous step) are sent to the recovered population after every iteration. It is known that there is a risk of reinfection(PREINFECTION). A person belonging to this population could therefore be reinfected at any iteration if it satisfies the criteria of reinfection. As people may be isolated, as though they were pursuing suggestions of social distancing, another scenario must be considered. For the sake of convenience, an isolated individual is assumed to be sent to the restored population when the probability of isolation is met. (PISOLATION).
(3) **A new population of infected individuals**. According to the protocol mentioned in the previous steps, this population collects all individuals infected at each iteration. At each iteration, it is likely that replicated new infected individuals are produced and it is thus suggested that such repetitive individuals are removed from this population before the next iteration starts running.

Step 4. **Stop Criterion**. The opportunity to terminate without the need to monitor any parameter is one of the most interesting aspects of the proposed solution. This condition happens because, as time passes, the recovered and dead populations are continuously increasing, and the current infected population does not infect new people. The number of infected individuals within a given number of iterations is expected to rise. However, from a specific iteration forward, because recovered and dead populations are so large and the scale of the infected population decreases gradually, the size of the current infected population would be less than that of the present size. In addition, a preset number of iterations (PANDAMICDURATION) can be applied to the stop criterion. Social distancing steps are also helping to meet the stop criteria.

2.9 Pseudocodes

The pseudocode of the most important functions for the CVOA is given in this section, along with some comments to better understand them [46].

2.10 CVOA Role

This is the key function and its pseudocode can be found in ***Algorithm 1***, It is important to maintain four lists: dead, recovered, infected (the existing set of infected people) and new infected peoples (the set of new infected people created by the spread of coronavirus from the current infected people).

The initial population is generated by using patient zero (PZ), which is a random solution, the number of iterations is regulated by the main loop; the duration of the pandemic is assessed (preset value) to determine if any infected person is still present. Each person will either die (it is sent to the dead list) or infect in this loop, thereby expanding the size of the new infected population. This infection process is encoded in the infection function (refer to section on infection function).

If the new population is created, all individuals are evaluated, and the latter is revised if any of them outperforms the best present one [46].

Algorithm 1 Function***cvoa***

1: **define**infectedPopulation, newInfectedPopulation, aux as set of *Individual*
2: **define** dead, recovered as *list* of *Individual*
3: **define** PZ, bestIndividual, currentBestIndividual, as *Individual*
4: **define** time as *integer*
5: **define**bestSolutionFitness, currentbestFitness as *real*
6: time ⟵0
7: PZ⟵ InfectPatientZero ()
8: infectedPopulation ⟵ PZ
9: bestIndividual ⟵ PZ
10: **while** time < EPIDEMIC_DURATION AND size of(infectedPopulation) > 0 **do**
11: dead die(infectedPopulation)
12: **for all** *i* ∈ *infectedPopulation* **do**
13: aux ⟵ infect (i, recovered, dead)
14: **ifnotnull**(aux) **then**
15: newInfectedPopulation aux
16: **end if**
17: **end for**
18:currentBestIndividual ⟵ selectBestIndividual (newInfectedPopulation)
19: **if** fitness (currentBestIndividual) >bestIndividual **then**
20: bestIndividual ⟵ currentBestIndividual
21: **end if**
22: recovered⟵ infectedPopulation
23: **clear**(infectedPopulation)
24:infectedPopulation ⟵ newInfectedPopulation
25: time⟵ time + 1
26: **end while**
27: **return** bestIndividual

2.11 Infect function

This function receives an infected person and returns the set of new people that are infected. Two additional lists, recovered and dead, are also collected as input parameters, as they must be modified after all infected individuals have been tested. In ***Algorithm 2***, the pseudocode is shown.

To evaluate the number of new infected individuals (use of SPREADER_RATE or SUPERSPREADER_RATE) or how distinct the new individuals will be (ORDINARY_RATE or TRAVELER_RATE), two criteria are evaluated. In the *newInfection* function, implementation of how these new infected individuals are encoded according to certain rates is carried out [46].

Algorithm 2 Function ***infect***

Require: infected as of *Individual*; recovered, dead as *list* of *Individual*
1: **define** R1, R2 as *real*
2: **define***newInfected* as *list* of *Individual*
3: R1 ⟵ RandomNumber()
4: R2 ⟵ RandomNumber()
5: if R1 <*P_TRAV EL* **then**
6: if R2 <*P_SUPERSPREADER* **then**
7: newInfected ⟵ newInfection (infected, recovered, dead, *SPREADER _RATE, ORDINARY_RATE*)
8: **else**
9: newInfected ⟵ newInfection (infected, recovered, dead, *SUPERSPREADER RATE, ORDINARY RATE*)
10: **end if**
11: **else**
12: if R2 <*P_SUPERSPREADER* then
13: newInfected ⟵newInfection (infected, recovered, dead, *SPREADER RATE, TRAV ELER RATE*)
14: **else**
15: newInfected⟵newInfection (infected, recovered, dead, *SUPERSPREADER RATE, TRAV ELER RATE*)
16**:** **end if**
17: **end if**
18: **return** newInfected

2.12 NewInfection Function

Provided a person is infected, based on the spreading and traveling rates, this function produces new infected individuals. This function also controls when new infected individuals are not already on the dead list (in such cases, this new infection is ignored) or on the recovered list (in such cases, this function is used to decide whether the individual is reinfected or stays on the recovered list). It

also assumes that the new potential infected individual may be isolated, and is managed by (by what)?. Although it was possible to incorporate the use of an additional list, it was agreed to treat these people as recovered. Therefore, if it is attempted to infect an isolated individual, it is added to the recovered list.

You will find the pseudocode for the mentioned procedure in *Algorithm 3*[45].

Algorithm 3 Function ***newInfection***

Require: infected as *Individual*; recovered, dead as *list* of *Individual*
1: **define** R3, R4 as *real*
2: **define** newInfected as *list* of *Individual*
3: R1 ← RandomNumber ()
4: R2 ← RandomNumber ()
5: aux ← replicate (infected, SPREAD_RATE, TRAV ELER_RATE)
6: **for all** i∈*aux***do**
7: if i∉ dead **then**
8: if i∉ recovered then
9: if R4 > P_ISOLATION **then**
10: newInfected ← i
11: **else**
12: recovered ← i
13: **end if**
14: else if R3 < P_REINFECTION **then**
15: newInfected ← i
16: **remove** i **from** recovered
17: **end if**
18: **end if**
19: **end for**
20: **return** newInfected

2.13 Die function

This function is named after the primary function. It assesses all individuals in the infected population and decides, based on whether or not they die. Those satisfying this criterion are sent to the dead list. This method is defined by *Algorithm 4*[46].

Algorithm 4 Function***die***

Require: infectedPopulation as *list* of *Individual*
1: **define** dead as *list* of *Individual*
2: **define** R5 as *real*
3: **for all**i∈ infectedPopulation **do**
4: R5 ← RandomNumber ()
5: **if** R5 < P_DIE **then**
6: dead i←
7: **end if**
8: **end for**
9: **return** dead

2.13 SelectBestIndividual Function

This is a secondary function used in a list of infected individuals to discover the best fitness. Its peudocode is presented in algorithm 5[46].

Algorithm 5 Function***selectBestIndividual***

Require: infectedPopulation as *list* of *Individual*
1: **define** bestIndividual as *Individual*
2: **define** bestFitness as *real*
3: bestFitness ← MINVALUE
4: **for all** i∈ infectedPopulation **do**
5: **if** fitness(i) >bestFitness **then**
6: bestFittness ← fitness(i)
7: bestIndividual ← i
8: **end if**
9: **end for**
10: **return** bestIndividual

3. Results and Discussions

3.1 Study Area and Description of Operational Scenario

The Gorgan-Roud catchment in Golestan province, Iran, is the case study included in this research. Voshmgir reservoir was chosen as a case study in this analysis. (The Gorganroud catchment in Golestan province, Iran, and Voshmgir Reservoir are the case studies included/chosen in this research).

Vashmgir Dam is located in Golestan province, 62 km northeast of Gorgan, on the Gorgan-Roud River. Its distance from the Caspian Sea is about 70 km and 24 km from the Iran and Turkmenistan border (figure 2). The volume of the reservoir is 46 and 54 million cubic meters at normal and overflow level, respectively.

In addition, the time from 2007 to 2019 was selected as the baseline period in the catchment, and the future interval is assumed as a 12-year interval (2040–2052).

The Bias Correction Spatial Disaggregation (BCSD) method of MIROC-ESM model was used to develop climate scenarios because its efficiency is appropriate in climatic model simulation.

In the first phase, by adding downscaled catchment climate data of the future interval, in the Extreme Learning Machine (ELM) model, the future runoff was simulated. Therefore, the ELM model was used to simulate the mechanism of rainfall-runoff in this research (figure 2).

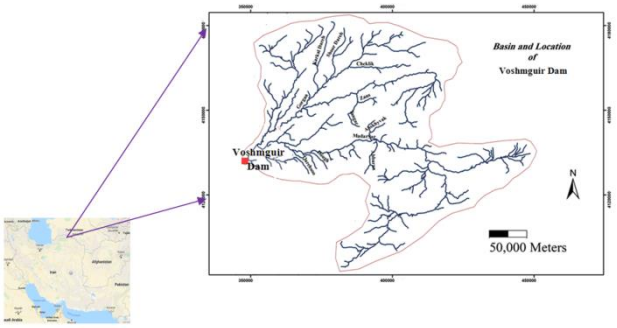

Fig. 2: location of Voshmgir dam (Northeast of Iran)

In the second phase, the amount of irrigation demand for the future period in various months was determined based on the climate data for the future period

In this research, to extract the operating rules from the Voshmgir Dam Single-Reservoir System in Northeastern Iran, the MOCOVA Meta-heuristic algorithm was developed.

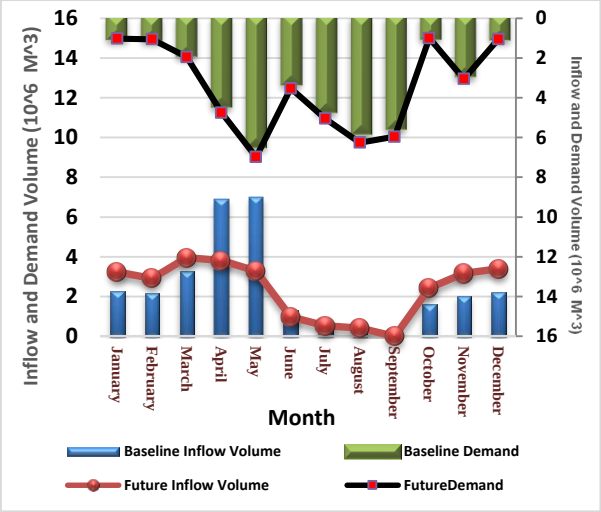

Fig. 3: Reservoir inflow and water demand volume under the baseline and climate change conditions

The reservoir surface-volume curve was derived using the following equation with the correlation coefficient R^2=0.968 and based on Fig.4.

$$Y = -0.002X^2 + 0.184X + 1.435 \quad (15)$$

The maximum water demand under the baseline and climate change conditions are 37.84 and 41.86 million cubic meters. The Reservoir inflow and water demand volume under the baseline and climate change conditions are shown in figure 3.

According to the research results, the ratio of water inflow to the reservoir under the climate change conditions would decrease by approximately 17% compared to baseline conditions. Therefore, the water demand ratio in such conditions would increase by 11%.

The optimum operating rules of the Voshmgir Dam reservoir were obtained by using the MOCOVA algorithm. The multi-objective problem included maximizing the model reliability and reducing its vulnerability.

The presumption of an 80% model reliability index indicates a clear difference between the vulnerability index values under the climate change and baseline conditions (figure 4).

Figure 3 reveals the effects of optimization algorithm as the Pareto curve for baseline and climate change conditions. It means that there will be 20% to 38% and 13% to 40% of vulnerability index changes in the baseline and climate change conditions, respectively.

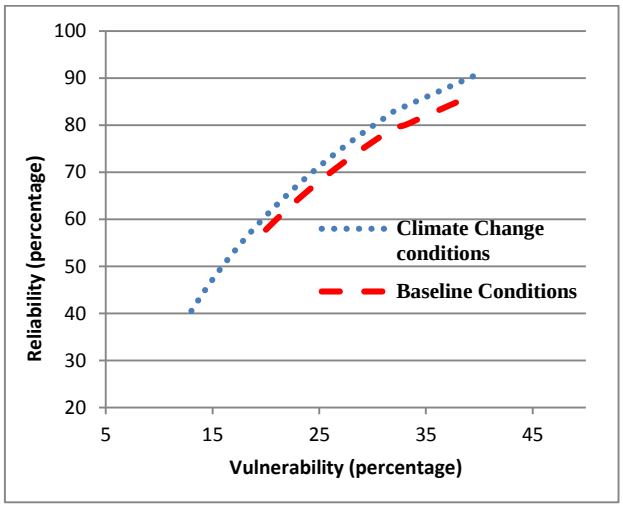

Fig. 4: Comparison of the vulnerability and reliability index of objective function under both conditions

The reliability index changes are 57% to 85% and 40% to 91% in both baseline and climate change conditions, respectively. In addition, 33% and 30% of vulnerability index will be generated for the reliability index of 80% under the baseline and climate change conditions, correspondingly. (Respectively has been repeated too many times).

As each point in the Pareto curve demonstrates a reservoir operation rule, including its vulnerability and reliability indices (Figure 4), none of the Pareto points have taken priority over others; in other words, they should vary depending on the catchment conditions and policies. The next step was to evaluate the optimal level of water demand rules under the baseline and climate change conditions.

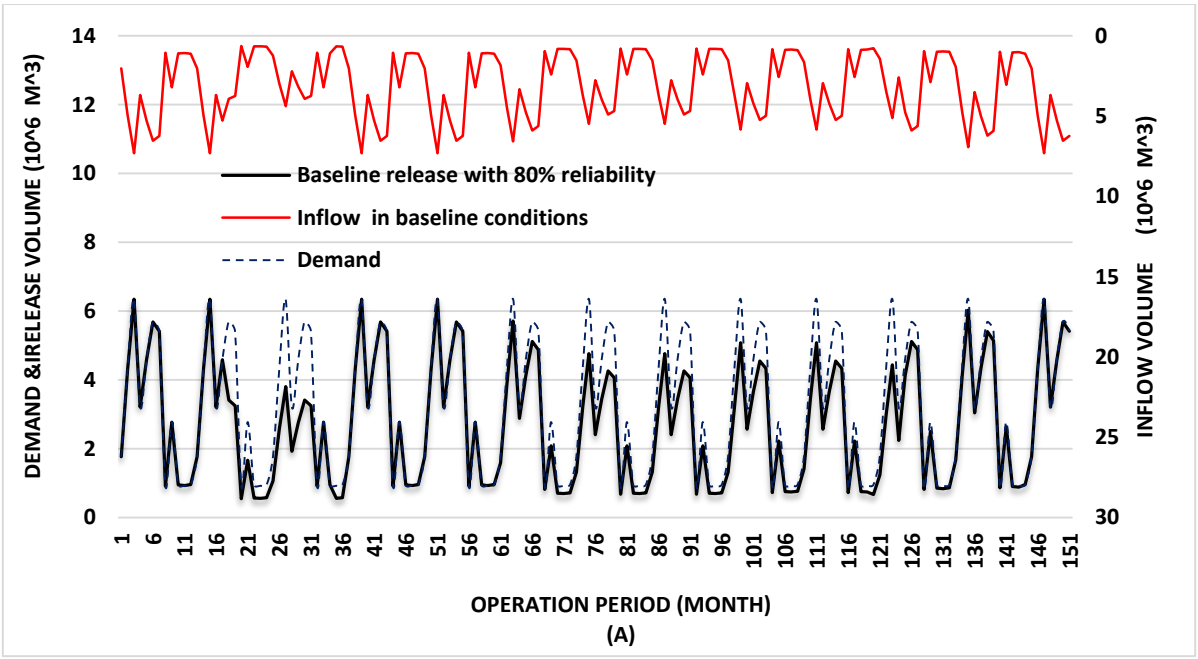

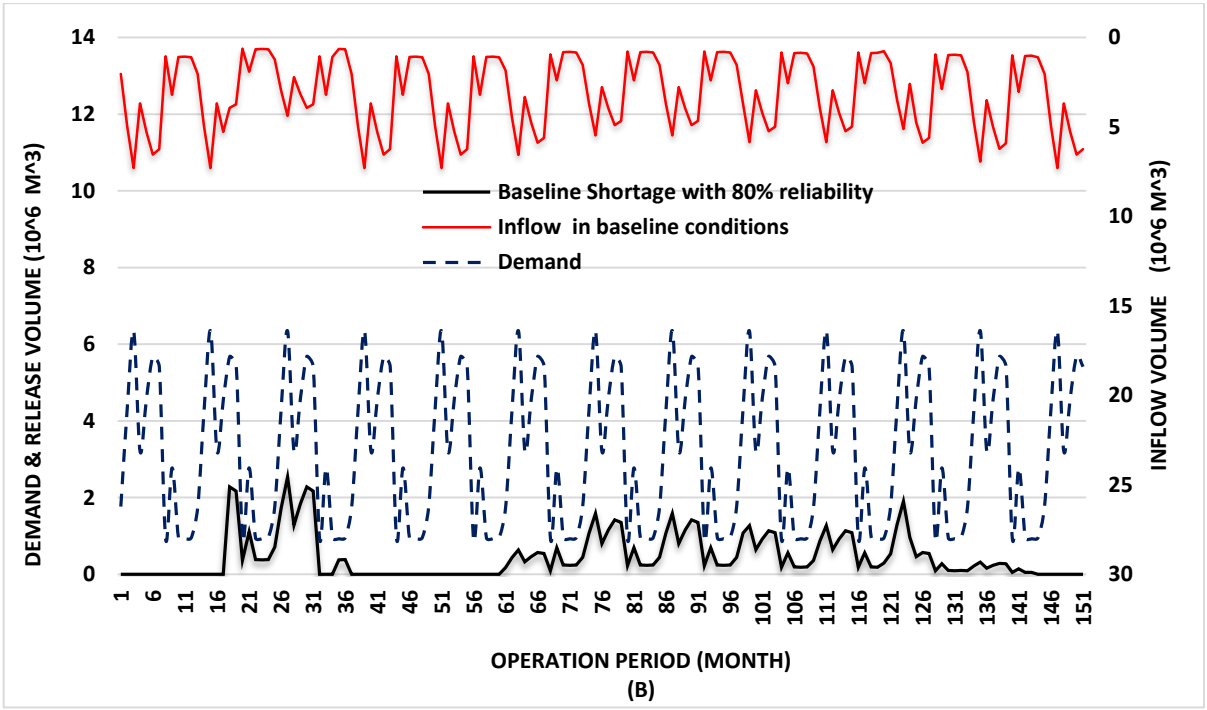

Fig. 5: comparison of (a) release volume (b) and shortage volume per each Pareto point resulted from 80% reliability under the baseline conditions

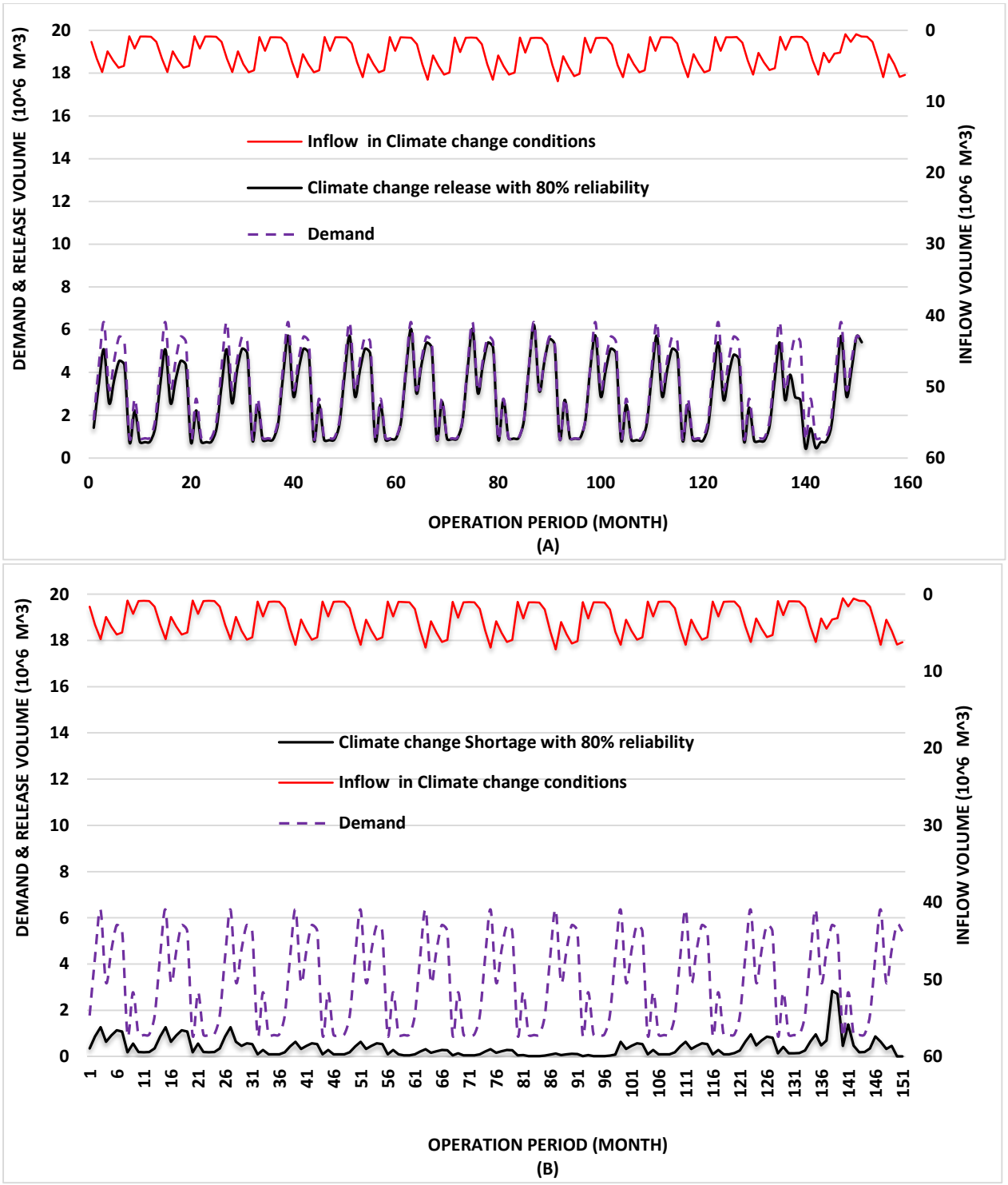

Fig. 6: comparison of (a) release volume (b) and shortage volume per each Pareto point resulted from 80% reliability under the climate change conditions

The baseline optimum rules were then compared to the optimum rules resulting under the conditions of climate change. On the other hand, Figure 3 indicates that the model vulnerability index values have been greatly decreased in all the values of common reliability between baseline and climate change conditions (i.e. 57% to 85%), which would make the model more reliable in climate change conditions. The effects of water demand supply for the 80% reliability index were recorded in figures 5a and 6a for the baseline and climate change conditions.

According to the corresponding demand for water, the following two alternatives were determined by the changes in shortages due to the optimum operating rules resulting from the proposed optimization algorithm, as seen earlier.

A correlation between the baseline and climate change conditions shows that the amount of reservoir water released is more consistent with the irrigation water demand under the climate change conditions. Moreover, the reservoir storage under the climate change conditions would be lower relative to baseline due to the increased release (figure 6b). The consequences are shown in (figure 5b) and (figure 5b), respectively.

According to (figure 5a) and (figure 6a), the climate change release rates of the reservoir are greater than those under the baseline conditions, which would be 11% due to increased demand for water under the climate change conditions.

On the other hand, (figure 5b) and (figure 6b) demonstrate that the performance of the dam has also increased under the conditions of climate change.

The objective function values of 80% reliability per Pareto point were determined in the next phase for evaluating the reservoir performance in supplying the downstream water demands, as defined in table 1. According to table 1, the reservoir release is more consistent with climate change conditions. Therefore, the dam efficiency is much higher due to the effects of climate change.

Table 1: comparison of objective functions in baseline and climate change conditions

Conditions	Reliability (%)	Vulnerability (%)
Baseline	80	33
Climate Change	80	30

It should be noted that the findings from this research are consistent with the findings of other studies, such as Ashofteh et al (2013) [39] and Donyaii et al (2020b) [30], that introduced the genetic programming and the farmland fertility optimization algorithm.

4. Conclusion

Studying the variation characteristics of streamflow and approximating the effects of climatic change are necessary for future water resources planning and management decisions. In water resources management, one of the greatest factors is to consider the priorities of all objectives within the policies regulating the operation of water resources systems to meet the needs for water. In addition, it is important to provide a set of alternative decision-making options (Pareto Curve) in such a way that executive managers can determine the relative value of the goals in this regard. It is also inevitable to extract multi-objective operational rules of reservoirs, as each point in the Pareto curve implies a reservoir operation rule that can be changed based on the favorite policies. The purpose of this study was to propose a specific guideline for the operation of such Pareto points, in order to decide how well these points could be applied in reservoir operation decision making, so that 80% of the downstream Voshmgir Dam agricultural lands in Iran would meet the water demand.

In this research, the climate change parameters such as temperature and precipitation values for baseline condition were first evaluated and then forecasted for the future period as the parameters of climate change conditions by the Bias Correction Spatial Disaggregation (BCSD) method of MIROC-ESM climatic model.

According to the results of all climate change scenarios, there will be an increase in the average monthly temperature up to 2.2 °C. In addition, a decrease of 23.8% in precipitation rate has been shown in the next period by evaluating the average monthly precipitation variations with respect to the baseline as an alert for the management of water supplies.

Afterwards, to evaluate the effect of climate change on the runoff flowing into the Voshmgir reservoir, the Extreme Learning Machine (ELM) model was used. Thus, by entering the output data of the climate change simulations into the ELM, the predicted rainfall-runoff data was determined. The findings showed that the amount of runoff would decrease to 0.87% under climate change conditions with respect to the baseline period.

Finally, the corona virus optimization algorithm (MOCVOA) was used to solve the problem of the reservoir system under the baseline and climate change conditions.

In order to obtain reservoir discharge rules (based on the Pareto curve), the two objective functions (i.e., maximizing the reliability index and minimizing the vulnerability index) were used based on parameters such as the flowing volume into the reservoir, the storage volume and the water demand volume obtained by the MOCVOA algorithm.

The research indicated that the vulnerability index variations under the baseline and climate change conditions were 20%to 38% and 13% to 40%, respectively. Furthermore, the

reliability index increase/surge/rise under the baseline and climate change conditions ranged from 57% to 85% and 40% to 91%, respectively. Meanwhile, for 80% reliability index of the model, the vulnerability ranged between 33% and 30% under the baseline and climate change conditions, correspondingly.

Thenceforth, in order to assess the performance of the reservoir in meeting the downstream water demand, the objective function values were compared to 80% of the reliability index in the aforementioned conditions. The findings indicate that the reservoir release rate is much more in line with the demand for climate change. -Thus, there is evidence that the Voshmgir Dam performs better under climate change conditions.

In other words, the study shows that all the values of common reliability between baseline and climate change conditions have substantially reduced the model vulnerability index values, which makes the model more stable under the conditions of climate change.

Acknowledgements

We hereby express our sincere thanks to the unit for conservation and operation of water resources of Golestan Regional Water Company for providing the data of Voshmgir Dam in line with this research.

References

[1] Huntington, T.G., 2006, "Evidence for intensification of the global water cycle: review and synthesis", J. Hydrol. 319: 83–95.

[2] Loaiciga, H.A., Valdes, J.B., Vogel, R., Garvey, J., Schwarz, H., 1996, "Global warming and the hydrologic cycle", J. Hydrol. 174: 83–127.

[3] Muzik, I., 2001, "Sensitivity of hydrologic systems to climate change", Can. Water Resour. J. 26: 233–252.

[4] Boyer, C., Chaumont, D., Chartier, I., Roy, A.G., 2010, "Impact of climate change on the hydrology of St. Lawrence tributaries", J. Hydrol. 384: 65–83.

[5] Bronstert, A., Kolokotronis, V., Schwandt, D., Straub, H., 2007, "Comparison and evaluation of regional climate scenarios for hydrological impact analysis: general scheme and application example", Int. J. Climatol. 27: 1579–1594.

[6] Jiang, T., Chen, Y.D., Xu, C.Y., Chen, X., Chen, X., Singh, V.P., 2007, "Comparison of hydrological impacts of climate change simulated by six hydrological models in the Dongjiang Basin, South China", J. Hydrol. 336: 316–333.

[7] Georgakakos, A.P., Yao, H., Kistenmacher, M., Georgakakos, K.P., Graham, N.E., Cheng, F.Y., Spencer, C., Shamir, E., 2012, "Value of adaptive water resources management in Northern California under climatic variability and change", Reservoir management, J. Hydrol. 412: 34–46.

[8] Hariri-Ardebili, M. A., Seyed-Kolbadi, S. M., V.E., Saouma, J. W. Salamon and Nuss, L. K. 2019, "Anatomy of the vibration characteristics in old arch dams by random field theory", Engineering Structures, 179(15): 460-475. doi.org/10.1016/j.engstruct.2018.10.082

[9] Yang, X.L., Gao, W.S., Shi, Q.H., Chen, F., Chu, Q.Q., 2013, "Impact of climate change on the water requirement of summer maize in the Huang-Huai-Hai farming region", Agric. Water Manag. 124: 20–27.

[10] Nam, W.H., Choi, J.Y., 2014, "Development of an irrigation vulnerability assessment model in agricultural reservoirs utilizing probability theory and reliability analysis", Agric. Water Manag. 142: 115–126.

[11] Mirzabozorg, H., Hariri-Ardebili, M.A.,Heshmati, M. and Seyed-Kolbadi, S.M., 2014, "Structural safety evaluation of Karun III Dam and calibration of its finite element model using instrumentation and site observation, Case Studies in Structural Engineering", 1: 6-12. doi.org/10.1016/j.csse.2014.02.001

[12] Loucks, D. P., and Van Beek, E., 2005, "Water resources systems planning and management: An introduction to methods, models and applications", UNESCO Publishing, Paris. MATLAB 9.0 [Computer software]. Natick, MA, MathWorks.

[13] Li, X., Guo, S.L., Liu, P., Chen, G.Y., 2010, "Dynamic control of flood limited water level for reservoir operation by considering inflow uncertainty", J. Hydrol. 391; 126– 134.

[14] Liu, P., Guo, S.L., Xu, X.W., Chen, J.H., 2011b, "Derivation of aggregation-based joint operating rule curves for cascade hydropower reservoirs", Water Resour. Manage. 25: 3177–3200.

[15] Liu, P., Li, L.P., Guo, S.L., Xiong, L.H., Zhang, W., Zhang, J.W., Xu, C.Y., 2015, "Optimal design of seasonal flood limited water levels and its application for the Three Gorges Reservoir". J. Hydrol. 527: 1045–1053.

[16] Vedula, S., Kumar, D.N., 1996, "An integrated model for optimal reservoir operation for irrigation of multiple crops", Water Resour. Res. 32: 1101–1108.

[17] Mujumdar, P.P., Ramesh, T.S.V., 1997, "Real-time reservoir operation for irrigation', Water Resour. Res. 33: 1157–1164.

[18] Umamahesh, N.V., Sreenivasulu, P., 1997, "Two-phase stochastic dynamic programming model for optimal operation of irrigation reservoir", Water Resour. Manage 11: 395–406.

[19] Hajilal, M.S., Rao, N.H., Sarma, P.B.S., 1998, "Real time operation of reservoir based canal irrigation systems". Agric. Water Manag. 38: 103–122.

[20] Haddad, O.B., Moradi, M.J., Mirmomeni, M., Kholghi, M.K., Marino, M.A., 2009, 'Optimal cultivation rules in multi-crop irrigation areas', Irrig. Drain. 58: 38–49.

[21] Consoli, S., Matarazzo, B., Pappalardo, N., 2008, "Operating rules of an irrigation purposes reservoir using multi-objective optimization", Water Resour. Manage 22: 551–564.

[22] Teixeira, A.D.S., Marino, M.A., 2002, "Coupled reservoir operation-irrigation scheduling by dynamic programming", J. Irrig. Drain. Eng. 128: 63–73.

[23] Prasad, A.S., Umamahesh, N.V., Viswanath, G.K., 2013, "Short-term real-time reservoir operation for irrigation", J. Water Resour. Plann. Manage. 139: 149–158.

[24] Reddy, M.J., Kumar, D.N., 2007, "Optimal reservoir operation for irrigation of multiple crops using elitist-mutated particle swarm optimization", Hydrol. Sci. J. 52; 686–701.

[25] Shnaydman, V.M., 1993, "The influence of climate variations on an irrigation water resources system performance strategy", Water Resour. Manage 7: 39–56.

[26] Georgiou, P.E., Papamichail, D.M., 2008, "Optimization model of an irrigation reservoir for water allocation and crop planning under various weather conditions", Irrig. Sci. 26: 487–504.

[27] Ncube, S.P., Makurira, H., Kaseke, E., Mhizha, A., 2011, "Reservoir operation under variable climate: case of Rozva Dam, Zimbabwe". Phys. Chem. Earth 36; 1112– 1119.

[28] Afkhamifar, S. and Sarraf, A. P., 2020, "Prediction of groundwater level in Urmia Plain aquifer using hybrid model of wavelet Transform-Extreme Learning Machine based on quantum particle swarm optimization", Watershed Engineering and Management, 12(2): 351-364. doi: 10.22092/ijwmse.2019.126515.1669, [in Persian].

[29] Donyaii, A. R., Sarraf, A. P. and Ahmadi, H., 2020a, "Water Reservoir Multi-Objective Optimal Operation Using Grey Wolf Optimizer", Shock and vibration journal., 1-10 https://doi.org/10.1155/2020/8870464

[30] Donyaii, A. R., Sarraf, A. P. and Ahmadi, H., 2020b, "Application of a New Approach in Optimizing the Operation of the Multi-Objective Reservoir", J. Hydraul. Struct., 6(3):1-20 DOI: 10.22055/jhs.2020.34556.1145.

[31] Ahmed KF., Wang G., Silander J., Wilson AM., Allen JM., Horton R. and Anyah R. 2013, "Statistical downscaling and bias correction of climate model outputs for climate change impact assessment in the US northeast", Journal of Global and Planetary Change", 100: 320-332.

[32] Huang GB., Liang NY. and Rong HJ., 2005, "On-line sequential extreme learning machine" In: The IASTED international conference on computational intelligence. Calgary

[33] Guo RF., Huang GB. and Lin QP., 2009, "Error minimized extreme learning machine with growth of hidden nodes and incremental learning", IEEE Trans Neural Netw 20(8):1352–1357

[34] Zhu QY., Qin AK. amdSuganthan, PN., 2005, "Evolutionary extreme learning machine", Pattern Recogn", 38(10):1759–1763

[35] Huang GB. and Siew CK., 2005, "Extreme learning machine with randomly assigned RBF Kernels", Int J Inf Technol 11(1):16–24

[36] Huang GB., Lei C. and Siew CK., 2006, "Universal approximation using incremental constructive feed forward networks with random hidden nodes", IEEE Trans Neural Netw 17(4):879–892

[37] Ding S., Guo L. amd Hou Y., 2017, "Extreme learning machine with kernel model based on deep learning, Neural Computing and Applications", 28(8):1975-84.

[38] Shokri A., Bozorg Haddad O., and Mari˜no M. A., 2013, "Algorithm for increasing the speed of evolutionary optimization and its accuracy in multi-objective problems", Water Resour. Manage. 27(7): 2231–2249.

[39] Ashofteh P.S., Bozorg Haddad O. and Mari˜no, M.A., 2013, "Climate change impact on reservoir performance indices in agricultural water supply", Journal of Irrigation and Drainage Engineering, 139(2):19434774.

[40] Karamouz M., Houck M. H. and Delleur, J.W., 1992, "Optimization and simulation of multiple reservoir systems", J. Water Resour. Plann. Manage. 71: 71–81. 10.1061/(ASCE)0733-9496(1992)118%3A1.

[41] Velavan TP, Meyer CG., 2020,"The COVID-19 epidemic",Trop Med Int Health, 25:278–280.

[42] Giordano G., BlanchiniF. and Bruno R., 2020, "Modeling the COVID-19 epidemic and implementation of population-wide interventions in Italy", Nat Med. 26: 855–860.

[43] Del Ser J., OsabaE. and Molina D., 2019, "Bio-inspired computation: Where we stand and what's next", SwarmEvolComput**.** 48: 220–250.

[44]. Boussaïd I., LepagnotJ. and Siarry P. ,2013, "A survey on optimization metaheuristics", Inf Sci**.;**237:82–117

[45] World Health Organization. 2019, "Available online athttps://www.who.int/es/emergencies/diseases/novel-coronavirus-2019" (last accessed March20).

[46] Martínez-Álvarez, F., Asencio-Cortés, G., Torres, J. F. , Gutiérrez-Avilés, D., Melgar-García, L. and Pérez-Chacón, R., 2020, "Coronavirus Optimization Algorithm: A Bioinspired Metaheuristic Based on the COVID-19 Propagation Model", Big Data, 8(4) .https://doi.org/10.1089/big.2020.0051